

## Automated computer-aided diagnosis of splenic lesions due to abdominal trauma

Teomete U<sup>1</sup>, Tulum G<sup>2</sup>, Ergin T<sup>3</sup>, Cuce F<sup>3</sup>, Koksall M<sup>5</sup>, Dandin<sup>4</sup> O, Osman O<sup>2</sup>

<sup>1</sup>Department of Radiology, Sparrow Health System, Michigan, USA

<sup>2</sup>Department of Electrical and Electronics Eng, Istanbul Arel University, Istanbul

<sup>3</sup>Department of Radiology

<sup>4</sup>Department of General Surgery

Gulhane Research and Training Hospital

<sup>5</sup>Department of Radiology, Ankara Numune Training and Research Hospital  
Ankara, Turkey

### Abstract:

**Background:** Computer-aided detection in the setting of trauma presents unique challenges due to variations in shape and attenuation of the injured organs based on the timing and severity of the injury. We developed and validated an automated computer-aided diagnosis algorithm to detect splenic lesions such as laceration, contusion, subcapsular hematoma, perisplenic hematoma, and active extravasation using computed tomography (CT) images in patients sustaining blunt or penetrating abdominal trauma.

**Methods:** We categorized the splenic pathologies into three groups: contusion/laceration, hematoma, and active extravasation. We first analyzed the spleen and perisplenic region by estimating the mean value and standard deviation of the spleen. We determined adaptive threshold values based on the histogram of the area and detected the lesions after morphological operations and volumetric comparisons.

**Results:** The overall performance of the three computer-aided diagnosis (CAD) algorithms is an accuracy of 0.80, sensitivity of 0.95, specificity of 0.67, and a diagnostic odds ratio (DOR) of 40 with a 95 % confidence interval (CI): 14 to 117. The CAD of perisplenic hematoma had the highest diagnosis rates with an accuracy of 0.90, a sensitivity of 0.95, specificity of 0.80, and DOR of 76 with a 95 % CI: 13 to 442.

**Conclusions:** We developed a new algorithm to detect post-traumatic splenic lesions automatically and with high accuracy. Our method could potentially lead to the automated diagnosis of all traumatic abdominal pathologies.

HIPPOKRATIA 2018, 22(2): 80-85

**Keywords:** Trauma, solid organ injuries, computer-aided diagnosis

**Corresponding author:** Uygur Teomete, Department of Radiology, Sparrow Health System, 1215 E Michigan Ave Lansing, MI 48912 USA, tel: +13052981617, e-mail: uteomete@gmail.com

### Introduction

Trauma is the most frequent cause of mortality and morbidity<sup>1,2</sup> among all age groups and is the leading cause of death before the age of 40<sup>3</sup>. Trauma poses a crucial universal health problem for all socioeconomic classes<sup>4,5</sup>. The abdomen ranks as the third most common site of injury following trauma. The spleen is the most commonly injured solid organ. Surgical exploration rate following abdominal trauma is 25 %<sup>6,7</sup>. The death rate following blunt or penetrating trauma varies between seven and ten per cent<sup>8,9</sup>. In a study of Hildebrand, severe intraperitoneal bleeding due to multi-organ trauma was found to be the most common reason for early deaths. They reported a mortality rate of 42 % due to blunt abdominal injury<sup>10</sup>. Although various diagnostic methods are used to detect intraperitoneal traumatic lesions, computed tomography (CT) is a more specific and sensitive diagnostic tool in

trauma patients compared to conventional radiography or ultrasonography<sup>11-15</sup>.

Computer-aided artificial intelligence systems have been evolving from experimental to clinical applications and implementations in radiology over the last decade. Especially rapidly improving the performance of the deep learning techniques will make them powerful tools for segmentation<sup>16,17</sup>, classification<sup>18,19</sup>, lesion/nodule detection<sup>20,21</sup>, and computer-aided diagnosis (CAD)<sup>22,23</sup> systems. By taking advantage of these innovations, radiologists can increase diagnostic accuracy in their interpretations with fewer false positives and identify lesion/nodule patterns that may easily evade from human eyes. Also, these computer-aided systems can aid the automated detection of repetitive tasks such as nodule detection.

The CAD has a powerful potential to streamline the radiologic diagnosis in the emergency department, where

a rapid and accurate diagnosis can be lifesaving. In busy emergency departments with high patient volume, issues with timely availability of the radiologist, and turnaround time for the radiologic diagnosis may significantly affect patient outcome. In our previous work, the only study in the literature using traumatized spleens, we introduced a new method for automated computer-aided segmentation of the injured spleen due to blunt or penetrating abdominal trauma with high accuracy<sup>24</sup>. The proposed method efficiently overcame challenges such as shape and density differences of the spleen on CT images.

We aim to develop and validate a robust method detecting traumatic splenic lesions such as laceration, contusion, perisplenic fluid, and active extravasation.

## Materials and Methods

### Study population and assessment of the CT images

Institutional Review Board (IRB) of the University of Ankara Numune Training and Research Hospital (IRB No E-16-1143/2016, 14/12/2016) approved this study and waived the requirement for informed consent due to the retrospective study design. We collected data of thirty-six patients presenting to the emergency department sustaining abdominal trauma between January 2017 and April 2018. We excluded four subjects younger than 18 years of age (motor vehicle accident) and two with image motion artifacts from this study. Our study group consisted of thirty subjects sustaining blunt and penetrating abdominal trauma who underwent abdominal CT scans.

We used a standardized CT scanning protocol for patients with abdominal trauma. CT scans were acquired when the subjects were hemodynamically stable. The CT studies were performed on Toshiba Aquilion 64 multidetector CT scanner (Toshiba America Medical Systems, Tustin, CA, USA). One hundred mL of intravenous contrast was administered using a power injector (Ulrich GmbH & Co., Ulm, Germany) in the arterial followed by portal venous phases using 3 mm slice thickness. Organ Injury Scale standardized by the American Association for the Surgery of Trauma (1994) was used to grade splenic injury using CT.

Three radiologists with over ten years of experience (Cuce F, Ergin T, Koksall M) had access to the patients' history and status on initial admission but were blinded to the surgical report, follow up and outcome details as well as official CT report. They manually drew the splenic contours independently and made the final segmentation decision in agreement. They also detected and documented the associated pathologic findings, first individually and then in agreement. Inter-observer variability of manual segmentation of splenic contours and splenic pathologies were 0.15 % and 0.23 %, respectively.

### Method of detection lesions with CAD

We categorized the traumatic splenic pathologies into three groups: contusion/laceration, hematoma, and active extravasation. We used the portal venous phase to detect contusion/laceration and hematoma while we used the ar-

terial phase to assess active extravasations. Segmentation of the spleen is the first step before the comprehensive detection of pathology. We developed a segmentation method for injured spleens in<sup>24</sup>, as the first step of this study with the performance of volume overlap of 89.6 %  $\pm$  9.73, dice coefficient of 93.6 %  $\pm$  2.97, precision of 90.13 %  $\pm$  4.32, and sensitivity of 97.63 %  $\pm$  2.21; which was determined to be successful and sufficient to perform CAD of splenic pathologies.

### Detection of contusion/laceration

We used the binary images of the segmented spleen and the CT volume in the portal venous phase as the inputs of the system. While investigating the density distributions of the spleen and the perisplenic region, we observed that the density distributions exhibit two hills and the right hills represent the splenic parenchyma (Figure 1). We used the right half of the right hill to calculate the mean and standard deviation of splenic parenchyma density distribution. The peak of the hill indicates the mean value, while one-third of the right tail yields the standard deviation. The endpoint of the tail is determined to be the last point along the right tail corresponding to one-tenth of the peak value. We determined three threshold values and four labels based on the mean value and standard deviation. The pseudo code of the proposed thresholding method is as follows:

```



---


thr1 = 0
thr2 = mean - 1.5 * std
if thr2 < 55
  thr2 = 55
end
thr3 = mean + 2 * std


---



```

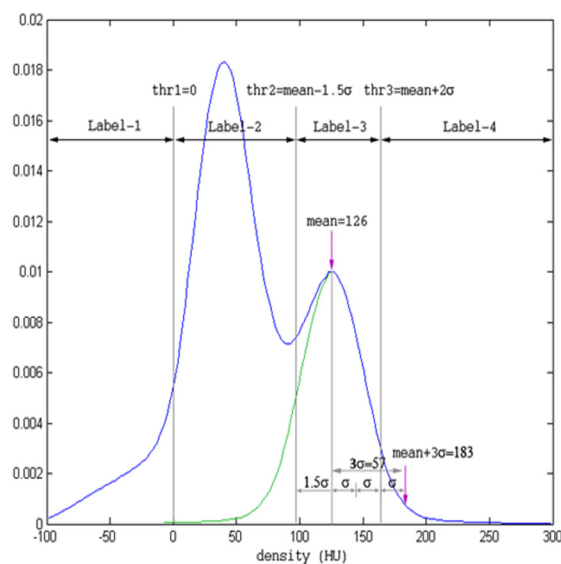


**Figure 1:** Determination of adaptive threshold levels from the histogram of the spleen and perisplenic region. The peak of the green hill, 126 Hounsfield unit (HU), depicts the mean value and one-third of the right tail indicates the standard deviation (std). Threshold values were determined as threshold 1 = 0, threshold 2 = mean - 1.5 x std, threshold 3 = mean + 2 x std.

The thresholding and labeling process, in one case is illustrated in Figure 1. The density of the peak value of the right hill, 126 HU, was taken as the mean value of the splenic parenchyma. One-tenth of the peak value corresponds to 183 HU on the right side, with a standard deviation  $s = 19$  HU. Label-3 indicated the density values of the spleen and designated between  $mean - 1.5s$  and  $mean + 2s$ .

The second label indicated probable laceration/contusion areas and was marked as red in Figure 2 for two slices. We applied morphological operations such as erosion, dilation, opening, and closing to reduce the small hypodense areas corresponding to artifacts.

Both sides of the vessel connections are the possible false positive regions that mimic laceration. Therefore, hyperdense areas at the medial part of the spleen were detected and subtracted followed by morphological dilation. We then analyzed the remaining portion of the second label and identified the connected components. We regarded components larger than 0.03 mL as contusion/laceration, while we classified others as an artifact.

#### Detection of perisplenic hematoma

To detect perisplenic hematoma, we first magnified the splenic volume in three dimensions using morphological operations; fourteen voxels in  $x$  and  $y$  Cartesian coordinates, one voxel to above the spleen and four voxels to under the spleen. Subtracting the original segmented splenic volume from the magnified splenic volume revealed the perisplenic region. We applied the same thresholding levels and selected label-2 as region of interest (ROI) for hematoma. As an example, two slices of a case is displayed in Figure 3. The first column shows the output of thresholding and labeling, and the second

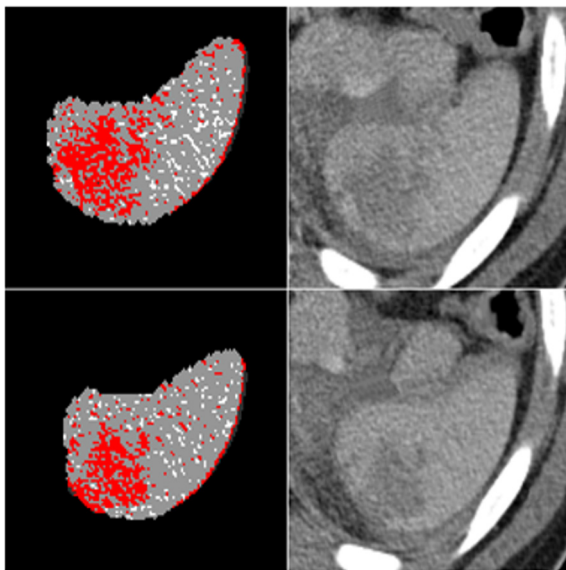


**Figure 2:** Thresholding and labeling processes of two different slices. Red regions indicate the label-2, the possible contusion/laceration areas.

column shows the original Digital Imaging and Communications in Medicine (DICOM) images with the label-2 indicated as green. After morphological operations, we performed a connected component analysis and calculated the volumes of each component.

Here, we encountered two possible scenarios for the location and the volume of a hematoma. In the first scenario, the hematoma is large and covers almost the entire circumference of the spleen. In the second, the hematoma volume is small and appears only posterior to the spleen. In the first scenario, the volume of the largest component has to be more than 4 mL to be labeled as a hematoma. Figure 3 is an example of the first case scenario. In the second case, the largest component is between 0.4 and 4 mL, and the centroid of the largest component must be posterior to the spleen. In these cases, the hematoma commonly accumulated in the posterior aspect of the spleen.

#### Detection of active extravasation

To detect active extravasation, we used arterial phase and segmented spleen volume. We defined active extravasation as a small group of pixels outside the segmented spleen. Therefore, relatively dense and large foci ( $>0.3$  mL) such as blood vessels, organs, and ribs were detected by connected component analysis followed by thresholding, using  $mean - 0.5s$  as a level of threshold. Then these areas were removed, and only small and dense particles remained. In Figure 4, white areas indicate the regions higher than the threshold level,  $mean - 0.5s$ . After removing large components and intersecting with enlarged and threshold spleen region, green pixels remained. Compo-

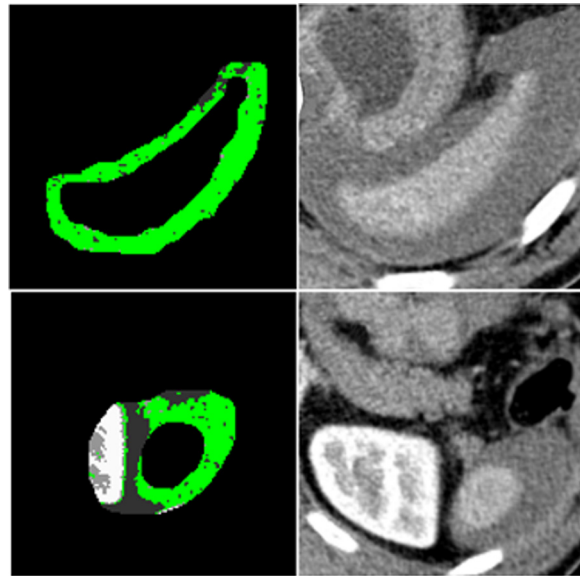


**Figure 3:** Subtracting the original segmented splenic volume from the enlarged spleen (fourteen voxels in  $x$  and  $y$  Cartesian coordinates, one voxel to above the spleen and four voxels to under the spleen) revealed the perisplenic region. After thresholding, label-2, highlighted in green, was assumed as the region of interest (ROI) for periorgan hematoma.

nents having density values higher than 190 HU and foci less than 0.3 mL in volume were considered active extravasation and indicated as red. In Figure 4, the original images are shown in the first column, possible foci of active extravasation near the spleen are shown in the second column in green, and the foci that meet the last condition are detected as active extravasation and indicated in red, shown in the third column.

## Results

We tested our proposed method in thirty subjects.

Twenty subjects had splenic trauma, and ten had other blunt organ traumas. Laceration/contusion was present in eighteen subjects; active extravasation was present in four and perisplenic hematoma in twenty cases. We validated the performance of our CAD method by calculating the accuracy, sensitivity, specificity, positive predictive value (PPV), negative predictive value (NPV), positive likelihood ratio (LR+), negative likelihood ratio (LR-), and diagnostic odds ratio (DOR) within 95 % confidence interval as displayed in Table 1.

The accuracy value is a metric that counts all positive

**Table 1:** Diagnosis performance of laceration/contusion, active extravasation, perisplenic hematoma, and all pathologies for the proposed computer-aided diagnosis (CAD) methods. The diagnosis indicators of overall performance of the three CAD algorithms are given at the last row.

	Accuracy	Sensitivity	Specificity	Positive predictive value (PPV)	Negative predictive value (NPV)	positive likelihood ratio (LR+)	Negative likelihood ratio (LR-)	Diagnostic odds ratio (DOR)	95% confidence interval (95% CI)
Laceration/contusion	0.77	0.94	0.50	0.74	0.86	1.89	0.11	17	3 - 84
Active extravasation	0.73	1.00	0.69	0.33	1.00	3.25	0.00	20	4 - 96
Perisplenic hematoma	0.90	0.95	0.80	0.90	0.89	4.75	0.06	76	13 - 442
All pathologies	0.80	0.95	0.67	0.71	0.94	2.86	0.07	40	14 - 117

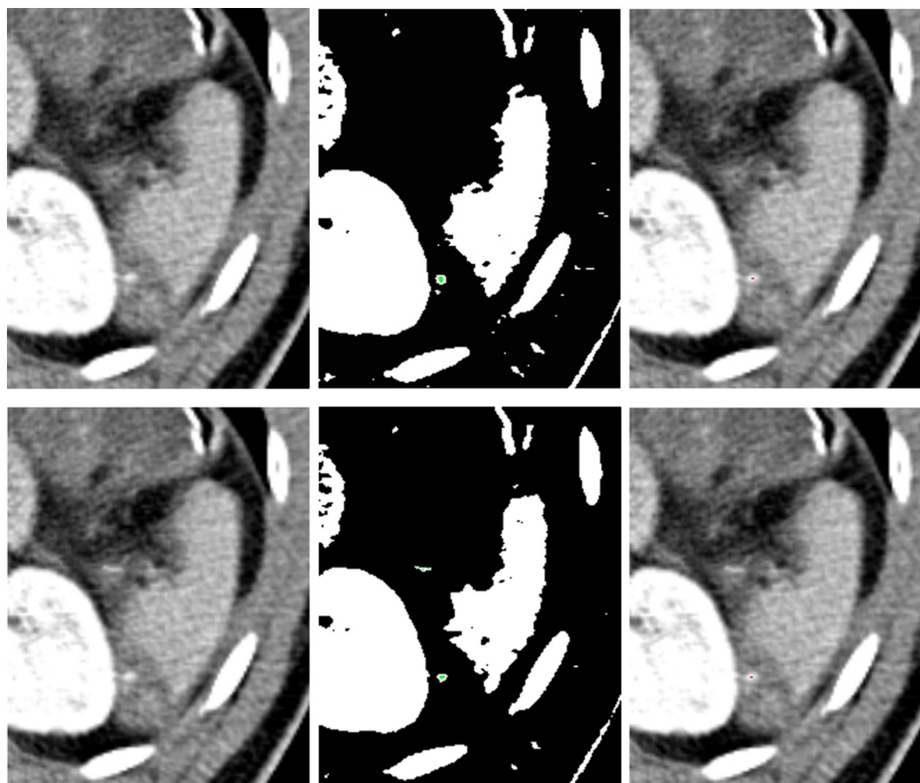


**Figure 4:** The first column: The original images. The second column: Possible active extravasation areas indicated in green. The third column: Detected active extravasation areas are indicated in red.

and negative predictions. According to Table 1, accuracies of all methods were between 73 % and 90 %, and the perisplenic hematoma diagnosis method had the highest accuracy. The specificity of the perisplenic hematoma diagnosis had the highest value of 80 %. The PPV of the detection method for active extravasation of 33 % was less than that of other methods because of relatively high false positive (FP) value and the low number of active extravasation cases. NPVs of all the three methods were high, and there was no false prediction among the subjects without active extravasation.

LR+ pertains to the degree of probability of disease when the test is positive. On the other hand, LR- is a measure of how much to decrease it when the test is negative. In diagnostic test results, LR+ values should be greater than one and LR- values should be less than one. In our test results, LR+ was between 1.89 - 4.75 and LR- was between 0.00 - 0.11.

For range estimates and significance testing, confidence intervals can be conventionally calculated using asymptotic standard error using the following formula<sup>25-27</sup>:

$$SE(\log DOR) = \sqrt{\frac{1}{TP} + \frac{1}{TN} + \frac{1}{FP} + \frac{1}{FN}} \quad (1)$$

where SE is the standard error. We then obtained the 95 % confidence interval of the log DOR by using the formula:

$$\log DOR \pm 1.96 SE(\log DOR) \quad (2)$$

We then obtained the confidence interval of the DOR by calculating the antilog of this expression.

DOR value of perisplenic hematoma diagnosis had the highest value with 76, indicating 76 times higher odds for positivity in subjects with perisplenic hematoma compared to odds for positivity among subjects without perisplenic hematoma.

Among these algorithms, CAD of perisplenic hematoma had the highest rates of diagnosis as evidenced by high true positive (TP) and true negative (TN) as well as low false positive (FP) and false negative (FN) values.

Indicators of overall performance of the three CAD algorithms are given at the last row of Table 1 as accuracy of 0.80, sensitivity of 0.95, specificity of 0.67, PPV of 0.71, NPV of 0.94, LR+ of 2.86, LR- of 0.07, and DOR of 40 with a range of 14 - 117, 95 % of CI.

## Discussion

Trauma is known as the leading cause of death before the age of 40, and overall is the fifth most common cause of mortality<sup>28</sup>. CT is crucial in the diagnosis of trauma. Successful diagnostic workup with CT, among other factors, also depends on the timely availability of a trauma radiologist. Delay in diagnosis or missed radiological findings can have significant consequences<sup>29</sup>. Discordant clinical outcomes may warrant repeated CT examinations, increasing patient's exposure to radiation, and iodinated contrast agent<sup>30</sup>. Eventually, the result is the loss

of time, a vital concern for trauma patients, as well as an increase in mortality and morbidity.

As an emerging technology, CAD systems have great potential for providing accurate and rapid detection of lesions automatically or semi-automatically from medical images. These systems can provide some additional information in daily clinical practice such as precise estimation of hematoma volume and intraperitoneal/intracavitary bleeding, along with correlation with the patient's hematocrit, assessment of viable or intact solid organ volume as well as the degree of the solid organ contusion and overall visceral perfusion. These systems can help radiologists detect subtle traumatic solid organ lesions and also help surgeons determine the operative or non-operative approach, surgery planning, and quantity of blood and fluid replacement.

In this study, we developed three CAD methods for automated diagnosis of contusion/laceration, hematoma, and active extravasation. We also obtained various performance metrics to validate developed methods. Our methods have a sensitivity of greater than 94 %. However, specificity values of the CAD of laceration/contusion and active extravasation were low due to a high number of false positives. Our method detected the small lacerations and contusions by applying low-level volumetric thresholds, resulting in a high false positive rate. The minuscule group of bright voxels in active extravasation makes detection difficult. Inhomogeneously enhancing segments of a thin vessel can be erroneously detected as active extravasation. We observed such segmentation errors, which increased both false positive rate and specificity. In cases of perisplenic hematoma detection, both sensitivity and specificity rates were high due to high TP rate combined with low FN and low FP rate coupled with high TN rate.

The PPV of the active extravasation diagnosis method was lower than other detection methods at 33 % because of the high FP rate and the small number of cases. NPVs of the three methods were high, and one for active extravasation, which means if the result is negative, it is correct in 100 % of the subjects.

LR+ and LR- values indicate the increase and decrease percentages for the probability of pathology detection. All LR+ values were greater than one, showing an increase in the likelihood of pathology diagnosis approximately between 15 % and 30 %. The LR- value decreases the probability of determination of pathology more than 45 %<sup>31</sup>.

DOR is an indicator of the effectiveness of a diagnostic test<sup>15</sup>. Odds for positive result among subjects with laceration/contusion is 17 times higher than the odds for a positive outcome in subjects with no laceration/contusion. The odds for a positive result in cases with active extravasation is 20 times higher than the odds for positivity among subjects with no active extravasation. Finally, the odds for a positive outcome among subjects with perisplenic hematoma is 76 times higher than the odds for positivity among subjects with no perisplenic hematoma.

Several other studies have been published about the segmentation of injured abdominal organs with limited cases. Davis ML et al, semi-automatically calculated from CT images the volume of thoracoabdominal injured organs following trauma<sup>32</sup>. Additionally, Rezaei et al presented a semi-automatic calculation of traumatized kidney volume with surrounding perirenal hematoma in 18 cases without detailed explanation, especially about the segmentation of fragmented kidneys due to trauma<sup>33</sup>. Danelson KA et al presented a study about semi-automatically measuring the grade of splenic injuries based on CT images and concluded that, with minimal data inputs from users, measurement of injury volume was feasible though their study involved only five injured spleens<sup>34</sup>.

To best of our knowledge, there is no study published about automated detection of splenic injuries in the English literature. Our proposed method can be further developed to determine all traumatic intraabdominal injuries from CT images automatically.

### Conflict of Interest

The authors declare no conflict of interest.

### References

- Berger LR, Mohan D. Injury control: A global view. Oxford University Press, Delhi, 1996, 1-34.
- Potenza BM, Hoyt DB, Coimbra R, Fortlage D, Holbrook T, Hollingsworth-Fridlund P, et al. The epidemiology of serious and fatal injury in San Diego County over an 11-year period. *J Trauma*. 2004; 56: 68-75.
- Baker S, O'neill B, Ginsburg M, Li G. The injury fact book. Oxford University Press, New York, 1992, 8-16.
- Aldemir M, Taçyıldız I, Girgin S. Predicting factors for mortality in the penetrating abdominal trauma. *Acta Chir Belg*. 2004; 104: 429-434.
- Hoyert DL, Xu J. Deaths: Preliminary data for 2011. *Natl Vital Stat Rep*. 2012; 61: 1-51.
- Townsend CM, Beauchamp RD, Evers BM, Mattox KL. Sabiston Text-Book of Surgery, the Biological Basis of Modern Surgical Practice. 18<sup>th</sup> edition. Elsevier-Saunders, Philadelphia, 2008, 512.
- Hemmila MR, Wahl WL. Management of the Injured Patient. Doherty GM (ed), Current surgical diagnosis and treatment. McGraw-Hill Medical, New York, 2008, 227-228.
- Fabian TC, Croce MA, Minard G, Bee TK, Cagiannos C, Miller PR, et al. Current issues in trauma. *Curr Probl Surg*. 2002; 39: 1160-1244.
- Karamercan A, Yilmaz TU, Karamercan MA, Aytac B. Blunt abdominal trauma: evaluation of diagnostic options and surgical outcomes. *Ulus Travma Acil Cerrahi Derg*. 2008; 14: 205-210.
- Hildebrand F, Winkler M, van Griensven M, Probst C, Musahl V, Krettek C, et al. Blunt abdominal trauma requiring laparotomy: an analysis of 342 polytraumatized patients. *Eur J Trauma*. 2006; 32: 430-438.
- ACEP Clinical Policies Committee, Clinical Policies Subcommittee on Acute Blunt Abdominal Trauma. Clinical policy: Critical issues in the evaluation of adult patients presenting to the emergency department with acute blunt abdominal trauma. *Ann Emerg Med*. 2004; 43: 278-290.
- Chiu WC, Cushing BM, Rodriguez A, Ho SM, Mirvis SE, Shanmuganathan K, et al. Abdominal injuries without hemoperitoneum: a potential limitation of focused abdominal sonography for trauma (FAST). *J Trauma*. 1997; 42: 617-625.
- Hauser CJ, Visvikis G, Hinrichs C, Eber CD, Cho K, Lavery RF, et al. Prospective validation of computed tomographic screening of the thoracolumbar spine in trauma. *J Trauma*. 2003; 55: 228-235.
- Poletti PA, Wintermark M, Schnyder P, Becker CD. Traumatic injuries: the role of imaging in the management of the poly-trauma victim (conservative expectation). *Eur Radiol*. 2002; 12: 969-978.
- Shanmuganathan K, Mirvis SE, Sherbourne CD, Chiu WC, Rodriguez A. Hemoperitoneum as the sole indicator of abdominal visceral injuries: a potential limitation of screening abdominal US for trauma. *Radiology*. 1999; 212: 423-430.
- Wang Y, Qiu Y, Thai T, Moore K, Liu H, Zheng B. A two-step convolutional neural network based computer-aided detection scheme for automatically segmenting adipose tissue volume depicting on CT images. *Comput Methods Programs Biomed*. 2017; 144: 97-104.
- Moeskops P, Viergever MA, Mendrik AM, de Vries LS, Benders MJ, Isgum I. Automatic Segmentation of MR Brain Images With a Convolutional Neural Network. *IEEE Trans Med Imaging*. 2016; 35: 1252-1261.
- Burns JE, Yao J, Muñoz H, Summers RM. Automated Detection, Localization, and Classification of Traumatic Vertebral Body Fractures in the Thoracic and Lumbar Spine at CT. *Radiology*. 2016; 278: 64-73.
- Anthimopoulos M, Christodoulidis S, Ebner L, Christe A, Mougiakakou S. Lung Pattern Classification for Interstitial Lung Diseases Using a Deep Convolutional Neural Network. *IEEE Trans Med Imaging*. 2016; 35: 1207-1216.
- Kooi T, Litjens G, van Ginneken B, Gubern-Mérida A, Sánchez CI, Mann R, et al. Large scale deep learning for computer aided detection of mammographic lesions. *Med Image Anal*. 2017; 35: 303-312.
- Setio AA, Ciompi F, Litjens G, Gerke P, Jacobs C, Van Riel SJ, et al. Pulmonary Nodule Detection in CT Images: False Positive Reduction Using Multi-View Convolutional Networks. *IEEE Trans Med Imaging*. 2016; 35: 1160-1169.
- Cheng JZ, Ni D, Chou YH, Qin J, Tiu CM, Chang YC, et al. Computer-Aided Diagnosis with Deep Learning Architecture: Applications to Breast Lesions in US Images and Pulmonary Nodules in CT Scans. *Sci Rep*. 2016; 6: 24454.
- Suk HI, Lee SW, Shen D, Alzheimer's Disease Neuroimaging Initiative. Deep ensemble learning of sparse regression models for brain disease diagnosis. *Med Image Anal*. 2017; 37:101-113.
- Dandin O, Teomete U, Osman O, Tulum G, Ergin T, Sabuncuoğlu MZ. Automated segmentation of the injured spleen. *Int J Comput Assist Radiol Surg*. 2016; 11: 351-368.
- Glas AS, Lijmer JG, Prins MH, Bossel GJ, Bossuyt PM. The diagnostic odds ratio: a single indicator of test performance. *J Clin Epidemiol*. 2003; 56: 1129-1135.
- Altman DG. Practical statistics for medical research. Chapman & Hall/ CRC, Florida, 1997, 229-276.
- Bland JM, Altman DG. Statistics notes. The odds ratio. *BMJ*. 2000; 320: 1468.
- Cherkasov M, Sitnikov V, Sarkisyan B, Degtiev O, Turbin M, Yakuba A. Laparoscopy versus laparotomy in the management of abdominal trauma. *Surg Endosc*. 2008; 22: 228-231.
- Sung CK, Kim KH. Missed injuries in abdominal trauma. *J Trauma*. 1996; 41: 276-282.
- Farach SM, Danielson PD, Amankwah EK, Chandler NM. Repeat computed tomography scans after pediatric trauma: results of an institutional effort to minimize radiation exposure. *Pediatr Surg Int*. 2015; 31: 1027-1033.
- McGee S. Simplifying likelihood ratios. *J Gen Intern Med*. 2002; 17: 646-649.
- Davis ML, Stitzel JD, Gayzik FS. Thoracoabdominal organ volumes for small women. *Traffic Inj Prev*. 2015; 16: 611-617.
- Rezaei P, Tochetto S, Galizia M, Yaghmai V. Perinephric hematoma: semi-automated quantification of volume on MDCT: a feasibility study. *Abdom Imaging*. 2011; 36: 222-227.
- Danelson KA, Hoth JJ, Miller PR, Stitzel JD. A semi-automated approach for measuring splenic injury using computed tomography. *Biomed Sci Instrum*. 2007; 43: 13-17.